Design and validation of a sensor guided robot control system for welding in shipbuilding

Mikael Fridenfalk, Gunnar S. Bolmsjö

Division of Robotics, Dept. of Mechanical Engineering
Lund University, Box 118
SE-221 00 Lund, Sweden

Abstract

New areas in welding large structures in shipbuilding include joining large sections such as double-hull constructions. Joining these sections create great problems for a manual welder since the welding takes place in a closed area with associated work environmental problems. The accessibility to the working area is limited to a man-hole and the use of robots for welding such structures requires new robot design that are adapted for the task as well as the additional requirements of one-off production.

This paper will describe research work and results within the ROWER-2 project. The aim of the project is to design a robot system for joining ship sections in the final stage when ship sections are to be assembled together in dry dock. Due to a high degree of manual work involved in the assembly procedure of the ship, the project addresses both productivity and quality issues. In addition, much welding operations are done in closed areas and the improvement of working conditions is of great importance as well.

An important part within the project is to develop control algorithms for seam tracking during welding. The aim is to be able to cope with tolerances in the joints after manual set-up and tack welding of the structure. The seam tracking method is based on the "through-arc" principle and development of the algorithms was made using simulation techniques. A special software system, FUSE, was developed for this purpose that seam-

lessly integrates commercial available software tools such as Matlab and Envision (robot simulator).

Experimentals were made in two stages. The first stage included detailed analysis and simulations to ensure a correct behavior of the seam tracking procedure during welding motions. This was followed by a first try-out using the real robot. The first try-out showed that the basic principles worked but some changes of the torch had to be made. The second stage included a theoretical up-date of the control algorithms followed by simulation based validation. A second try-out using the real robot showed results similar to those from simulations.

Simulation in FUSE showed that the major part of the development of sensor control algorithms should be performed by simulation, since it cuts time, expenses and efforts, especially when software simulation is included in the methodology.

1 Introduction

1.1 Robot welding

Since manual labor is a highly limited resource, especially when it comes to skilled craftsmen, robot automation is essential for future industrial expansion. One application area is presently robot welding, by which the welding quality and the environmental conditions for welders are improved and the productivity is increased. This applies especially to robot welding in shipbuilding [25, 23, 24] where large structures are welded, including the joining of large double-hull sections.

1.2 Seam tracking

Seam tracking [5, 7, 8, 12, 19] is essential for automation in shipbuilding for manufacturing of large passenger and cargo ships, such as supercruisers and oil-tankers, where high tolerances in the sheet material are allowed to minimize manufacturing costs.

A great number of Sensor Guided Robot Control (SGRC) systems for seam tracking at arc welding have been developed. The patents within this application area during the last 40 years indicates that a there is a clear tendency that old methods using mechanical, inductive, electrical and infrared sensors are becoming less important along with the use of

electron beams, cameras and optical lens systems. Today laser scanners and arc-sensors mainly replace these systems.

The difference between systems based on laser scanners and arc-sensors is accuracy, geometry and price. Laser scanners provide for a more accurate signal than arc-sensors, which contain much noise due to the interference of the welding process. On the other hand, laser scanners have to be mounted on the torch, decreasing the workspace of the robot. Laser scanners are also significantly more expensive than arc-sensors, which perhaps is one of the reasons why the majority of the patents that have been issued during the last 10 years within this application area [26, 3, 27, 17, 16] are based on through-arc sensing, while systems based on laser scanners are hardly even represented.

1.3 Process control

Besides the geometry of the seam, considerations has to be made in seam tracking of the process-related welding parameters [29, 1]. The welding process contains many parameters, such as the arc voltage, wire-speed and wire material. The aim is to determine feasible parameters for a welding procedure before seam tracking. This may be done by the performance of experiments or the use of knowledge based systems [4, 28]. If it is however not possible or desirable to keep these settings constant through the entire seam [14, 15, 18, 27], for instance due to the characteristics of the power-source, adaptive control may be introduced into the seam tracking procedure for maintaining the desired welding quality.

1.4 Through-arc sensing

The usual methods used for automated arc welding are gas metal arc welding (GMAW), flux-cored arc welding (FCAW) and submerged arc welding (SAW). In GMAW, metal parts are joined together by heating them with an arc established between a continuous, consumable filler metal electrode and the workpiece. The filler metal is either transferred to the workpiece in discrete drops under the influence of electromagnetic forces and gravity or in the form of molten electrode produced by repetitive short-circuiting.

Through-arc sensing was introduced in the beginning of the 80th and is described by among others G. E. Cook et al. [9]. According to experimental results, the approximate relationship between the arc voltage V, the arc current I and the nearest distance between the electrode and

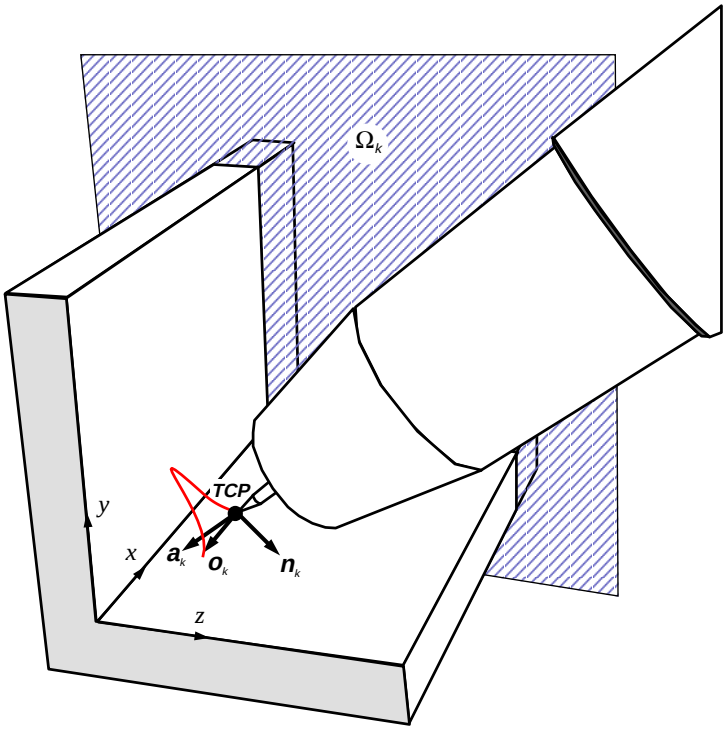

Figure 1: *Seam tracking setup. Definition of the coordinate systems of the workpiece and the Tool Center Point (TCP). The a_k is called the approach axis and coincides with the welding wire. Surface Ω_k is per definition always perpendicular to o_k.*

the workpiece l, may be expressed for an electrode extension ranging between 5-15 mm, by the equation:

$$V = \beta_1 I + \beta_2 + \beta_3 / I + \beta_4 l \tag{1}$$

where the constants $\beta_1 - \beta_4$ are dependent on factors such as wire, gas and power-source. Theoretically, if the power-source is adjusted for keeping the current at a constant level, and succeeds to do so, V will be a linear function of l. Practically, the voltage and current readings of the arc contain much noise, why the signal data has to be filtered by a low-pass filter.

In through-arc sensing, the welding is performed parallel to the seam-walls, see Fig. 1. By weaving the arc across the weld joint, the geometrical profile of the workpiece is obtained, since the distance from the tooltip perpendicular to the nearest wall is a function of the arc current and the voltage, as approximately expressed in Eq. 1.

1.5 Control algorithms for seam tracking

1.5.1 Template matching

The first suggested method in [9] is template matching. In this method the width and centering corrections are made proportional to e_a and e_n, where $t(x)$ and $s(x)$ are the template signal and the measured arc signal as a function of displacement x with respect to the center of the weld joint. The template signal is the measured arc current at welding, when the position of the workpiece is optimal. A denotes in Eq. 2 and 3 the weaving amplitude:

$$e_a = \int_{-A}^{A} |t(x) - s(x)| dx \tag{2}$$

$$e_n = \int_{-A}^{0} |t(x) - s(x)| dx - \int_{0}^{A} |t(x) - s(x)| dx \tag{3}$$

The template signal may here be analytically or empirically determined. Other examples of error calculations are by using the integrated difference and the integrated difference squared errors. Control in a and n-directions in Fig. 1 is performed by comparing the average value of $s(x)$ at, and near the weave center position with a reference value.

1.5.2 Differential control

The second method consists of differential control. It is computationally more simple and has proven to be quite reliable for control in a and n directions. Instead of sampling data during the whole weaving cycle, sampling is only made at the turning points in the weaving trajectory. Measuring the arc-signal, i.e. the current in the case of GMAW, FCAW or SAW, the vertical distance error e_a will be proportional to the difference between the average current sampled at the center of the oscillation $i(0)$, and the reference current value I_{ref}:

$$e_a = K_a[i(0) - I_{ref}] \tag{4}$$

In similar manner, the difference between the two samples is proportional to the magnitude of the cross-seam distance error e_n:

$$e_n = K_n[i_{+A} - i_{-A}] \tag{5}$$

where i_{+A} and i_{-A} are the average measured current at a pair of adjacent extreme points. The parameters K_a and K_n are dependent on the weld joint geometry and other process parameters such as shielding gas and wire feed rate. Since these parameters will be known in advance however, K_a and K_n may be defined for any welding application.

1.6 Simulation using virtual sensors

Virtual sensors are presently used in many application areas, such as robotics, aerospace and marine technologies [6, 10, 20, 22]. The development of new robot systems, such as for seam tracking may be accelerated by the application of simulation. In general the design methodology of virtual sensors may vary due to their specific characteristics. If the characteristics are not known for the design of analytical sensor models, artificial neural networks are sometimes used to make approximations of the behavior of the sensors [2, 21].

1.7 ROWER-2 application

The objective of the European ROWER-2 project was to automate the welding process in shipbuilding, more specifically for joining double-hull sections in supercruisers and oil tankers. According to the specifications the workers should be able to mount the robot system inside the cell and

supervise the welding-process from a remote distance. Every hull-cell should be equipped with a man-hole, through which the robot may be transported, see Fig. 2. Since the robot has to be transported manually, the constraints on the robot are that each part is not allowed to weigh more than 50 kg. Further on, the robot system should be designed to operate in standard hull-cells with predefined variations in dimension. To be able to meet the specifications, a robot manipulator was built based highly on aluminum alloy. The robot was mounted on a mobile platform with 1 degrees of freedom to increase its workspace.

Figure 2: *A double hull-cell in ROWER-2 with man-hole through which the robot equipment is manually transported. One of the walls and the floor have been excluded from the picture.*

The method chosen for automatic welding in the ROWER-2 project was GMAW using through the arc-sensing at seam tracking [9]. A simple seam tracking algorithm was developed at an early stage of the project [13]. By the application of the Flexible Unified Simulation Environment[1] (FUSE) [11], this algorithm was optimized and evolved into many new algorithms. They were initially designed to contain the basic functionality of the Yaskawa COM-ARC III sensor [30] but were further developed to meet the ROWER-2 and other specifications.

Since one of the simple algorithms showed by simulation to meet the

[1] An integrated software system based on Envision (robot simulator) and Matlab

ROWER-2 specifications, it was chosen for implementation in the project. The implementation was performed in C++, running on a QNX-based[2] embedded system. The algorithm was further developed to be able to handle long welds by using linear interpolation. A method was additionally developed to compensate for the power-source controller that interfered with the seam tracking process by disabling control in negative a-direction of the TCP. An automatic delay detection for synchronization between the control system and the data from the arc-sensor was also designed to secure the control in the n-direction of TCP.

[2]QNX is an operating system for embedded controllers.

2 Material and methods

2.1 Systems development methodology

The methodology is based on the assumption that software development in robotics is the part that requires most time, money and effort at development of robot systems. To optimize the procedure of robot design from virtual prototyping and systems development to the final integration of the robot in a production line, a new software system was designed that can be used during the whole process. FUSE fills the gap that traditionally exists between CAD/CAM/CAE, robot simulation systems and software simulation environments.

Figure 3 presents the methodology that was developed and used for the design and validation of a seam tracking algorithm in the ROWER-2 project. In this figure design of model denotes the design of a model that is focused on the functionality of the algorithm. Simulation and verification of the model denotes the process to estimate the potential and find the limitations of the algorithm. Software structure simulation is not bound to the model itself but to the implementation of the model at a later stage.

It is an awkward task to debug complex algorithms after they have implemented in the robot system. At an early development stage, however, a detailed simulation of the execution flow, supported by automatic testing programs will most likely isolate the problems. The test programs may be used to systematically find the limits of the algorithm and make sure that it behaves as expected.

Any significant change in the algorithm structure in the verification phase implies similar change in the simulation model of the software to mirror the program flow in the robot system. If the algorithm has been developed with care using software simulation to begin with, such modification will require minimal effort.

By physical validation, deficiencies may be found in the simulation model. If the specifications are not met, the model is modified and new model and program structure simulations are performed. When the specifications are met by physical validation, the process is terminated by a final evaluation of the simulation model using the optimized parameters found by physical validation.

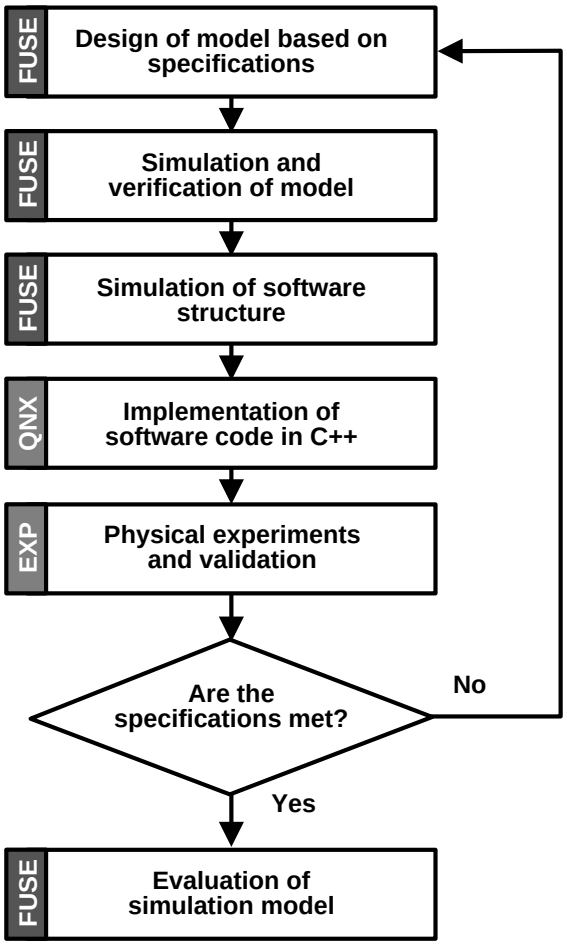

Figure 3: *The methodology developed for the design and physical validation of the seam tracking algorithm in the ROWER-2 project.*

2.2 Joint profiles

The simulation was performed on fillet and V-groove joints, according to the specifications in the ROWER-2 project. Due to the specifications, the algorithm had to be able to make compensations for a deviation of ±300 mm in y and z directions during a 15 m long weld (see Fig. 1 and 4 for the definition of the coordinate axes). This was redefined as a maximum deviation of ±20 mm per meter weld, or ±2% expressed in percentage. Profiles of fillet and V-groove joints are presented in Fig. 4. Since the start point of the seam is always found by image processing before seam tracking is performed, no special consideration has to be taken at start.

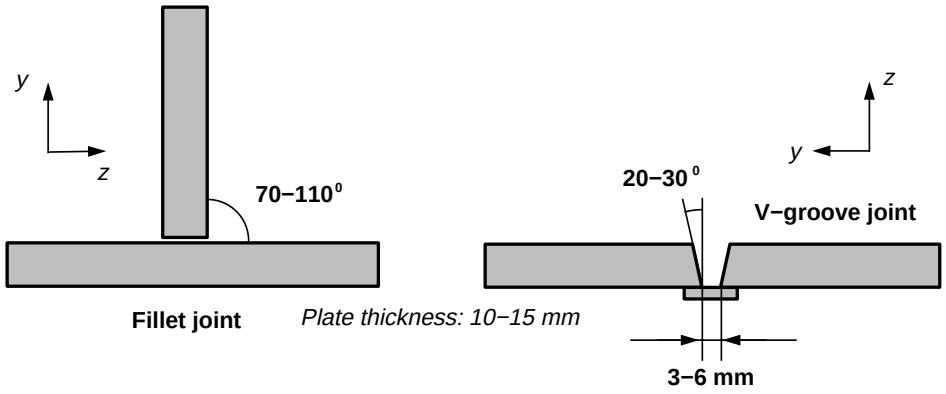

Figure 4: *Fillet and V-groove joints were used in simulation and physical validation. The lengths of the sample plates in the experiments were 600 mm (orthogonal to the plane of the figure).*

2.3 Experimental setup

The functionality of the seam tracking model and the essential features of the program structure were simulated in FUSE using SGI workstations and manually translated to C++ for implementation in the robot system running on QNX OS, using a real-time industrial PC. As power-source for welding, a Migatronic BDH STB Pulse Sync 400 for MIG/MAG was chosen operating together with a Planetics Mars-501 push-pull unit. According to specifications the push-pull unit is suited for welding cables up to 25 meters between the units and another 16 meters between the pull unit and the welding torch. OK Autrod 12.51 was used as welding wire

together with 80Ar/20CO_2 shielding gas. Figure 5 displays the ROWER-2 robot.

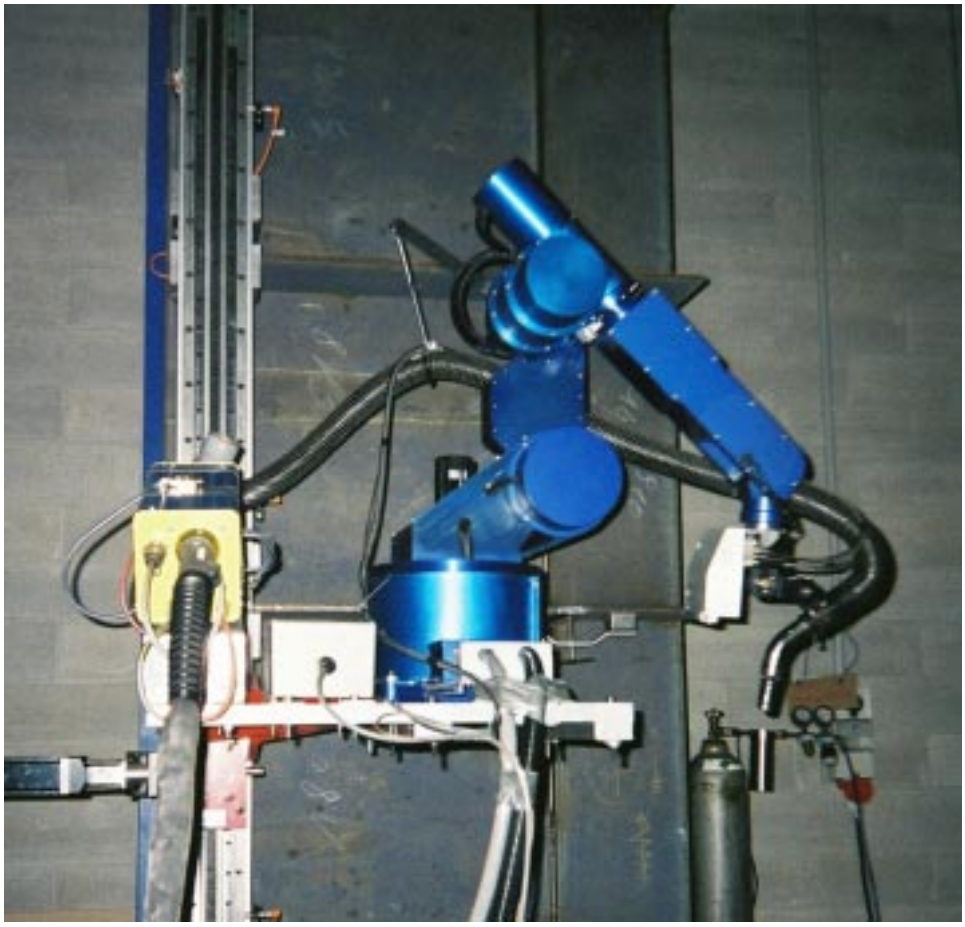

Figure 5: *The ROWER-2 robot system. The system is mounted on a mockup that is about 3.5 m high, belonging to the hull cell of a ship. The metallic box near the torch is a camera that is used to identify the start point of the seam.*

3 Experimental results

3.1 Simulation experiments

3.1.1 Overview

A number of seam tracking algorithms were developed and implemented in FUSE. The differential algorithm, which was considered to be the easiest one to implement and required the lowest amount o computational power yet satisfying the ROWER-2 specifications, was chosen for implementation and physical validation in the ROWER-2 project. The simulation and validation work presented in this section is based on the differential algorithm presented in the introduction.

3.1.2 FUSE simulations

The simulations in FUSE were performed using FUSE Wizard, see Fig. 6. The wizard lists the available algorithms and makes suggestion of parameters for the selected one before the start of the simulation.

The first algorithm in the wizard is a simple differential algorithm using distance measurements directly retrieved from the FUSE environment. This was an early prototype of the differential algorithm, but worked principally in the same way as the calibrated differential, implemented in the robot system.

The calibrated differential algorithm uses a virtual arc-sensor and is calibrated by FUSE Wizard. At calibration, the value of the main current is calculated and saved. The calibration value may be changed before the start of any new experiment. In simulation the same calibration value showed to work properly for both fillet and V-groove welds. In physical experiment however, different calibration values for fillet and V-groove welds were used for optimal performance.

The two last methods in the wizard input dialog are two algorithms that use statistical methods to find the 2D geometry of the seam, perpendicular to the direction of motion. The last algorithm is in addition able to adapt to the orientation of the joint perpendicular to the direction of motion by rotation of the TCP around the o-axis.

Initial simulations showed that the differential algorithm was theoretically able to meet the specifications. By physical experiments, the model was modified due to changes of parameters such as welding speed, weaving amplitude and frequency. These data, along with other data such as

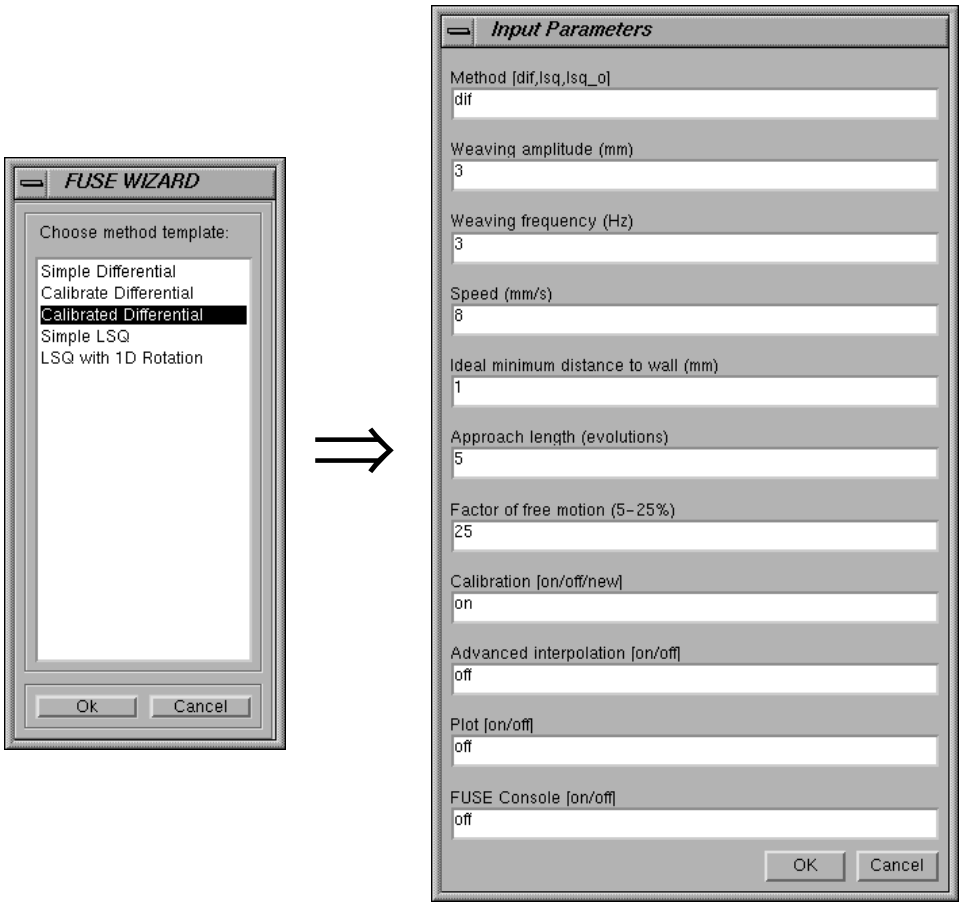

Figure 6: *The FUSE Wizard. For each algorithm a special set of parameters is suggested that may be modified by user input before simulation. New algorithms may be added or removed from the list throughout the development process.*

nominal voltage, were optimized by a series of tests performed by an experienced welding specialist tuning the welding system. To evaluate the simulation model compared to real experiments, a final series of simulations were performed using the power-source parameters that had shown to give high quality welds.

According to the evaluation, the theoretical limits for the algorithm is a deviation in the interval between –10% and 30% with $K_a = 0.01$ and $K_n = .005$. This is better than ±2% (specifications). The conclusion is that the ideal case, when the current has very low amount of noise, and Eq. 1 is valid, the maximum allowed deviation is ±20% (moving the offset of the nominal welding trajectory to the middle). The asymmetrical performance (–10% to 30%) is most likely related to the present control system. A closer study of this phenomenon was however never made.

Figures 7-17 present a few simulations performed for evaluation purpose after the verification of the algorithm by series of real experiments. In all these experiments, K_n were 50% of K_a, which is an empirically derived optimal value verified by robot welding experiments.

The criterion for a good weld is that the final result should at ocular examination be similar to a straight weld without seam tracking. To be able to produce such result, the instability that occurred during SGRC was minimized by using gains that made it possible to meet the specifications.

At too low gains, the algorithm does not make compensation enough to meet a specific deviation. On the other hand, if the gain is too large, instability will occur resulting in low welding quality. So the trick is to find the largest gains for K_a and K_n both at positive and negative deviations and both for fillet weld and V-groove welds at which the seam tracking remains stable and converges smoothly to the seam. At these gains the maximum possible deviations are found by experimentally increasing the deviation step by step until the algorithm has reached the limits of its performance.

3.1.3 Vector booster method

To increase the performance of the algorithm, a feature called the vector booster was implemented. The vector booster method consists of a pre-calculation of seam direction at the beginning of seam tracking and subsequent alteration of nominal trajectory according to the initial prognosis for the rest of the seam.

This method showed to increase the performance of the algorithm by a factor of up to two. The vector booster is not optimized for dealing

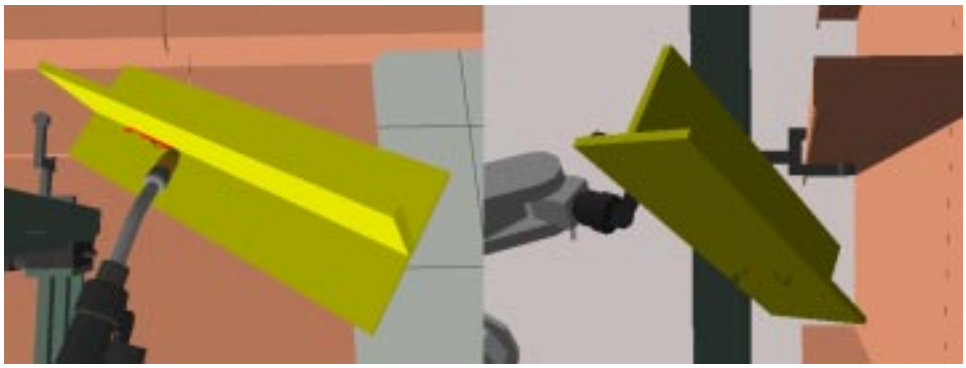

Figure 7: *Extreme deviations like this (60%) are not used in practice. According to specification, the algorithm has to handle a deviation of 2%, which is 30 times smaller than the one in the picture. The picture demonstrates however the effect of the vector booster, working especially well for large deviations. Although the simulation succeeded, A deviation of 30% or smaller is recommended using the vector booster for maximum quality of the weld.*

Figure 8: *The same experiment as in the previous figure. The vector booster showed to be of limited interest at moderate deviations. The method inspired however the design of the power-source compensation component in the algorithm, described later in this section.*

with small deviations, but rather extreme deviations, many times larger than the specifications, see Figs. 7-8.

The vector booster does theoretically increase the welding quality at large deviations, due to the need of lower gains in the SGRC system. With larger expected deviations, higher gains have to be set by the operator. And high SGRC gains may in turn decrease the welding quality due to higher instability at seam tracking, by causing small oscillations.

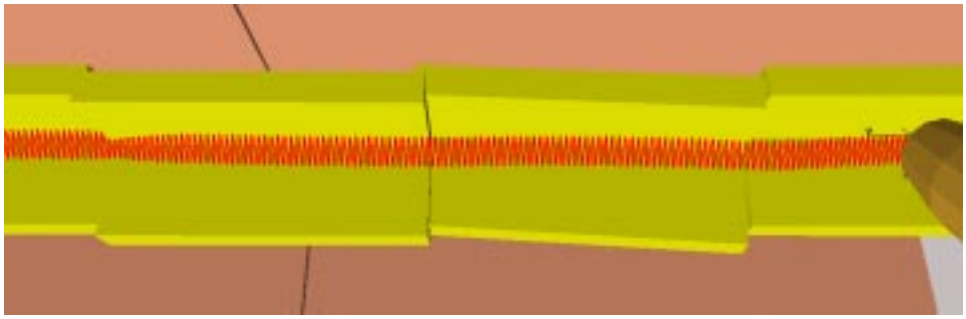

Figure 9: *The seam tracking algorithms were first developed using workpieces like this one.*

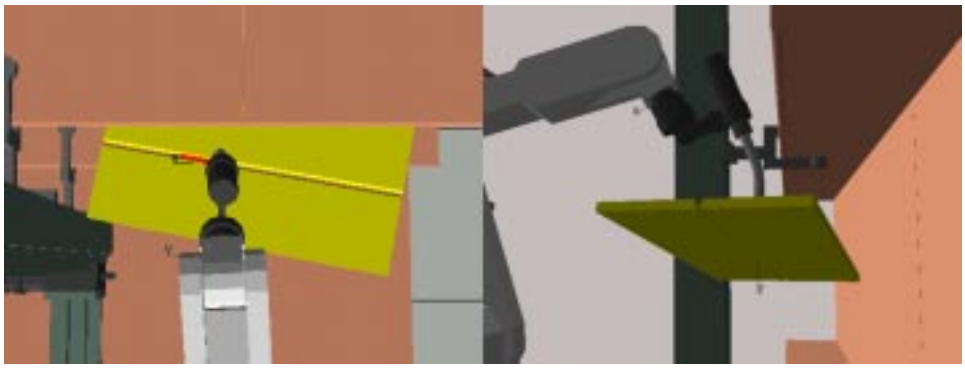

Figure 10: *At a later stage, when it turned out that all seams in practice were straight, only such workpieces were used for simulation experiments. A V-goove weld simulation is displayed in this picture.*

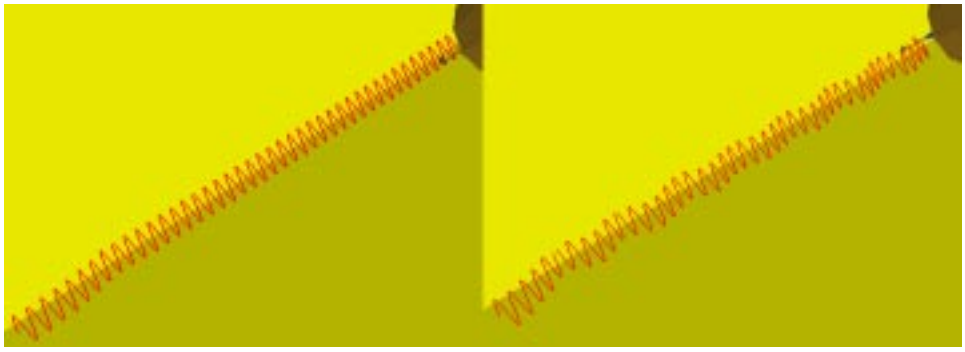

Figure 11: *Seam tracking with deviations by 30% in y and z directions, using the vector booster. Left: at K_a = 0.010 the seam tracking process is very stable, which is a prerequisite for high welding quality. Right: K_a = 0.020 gives high instability.*

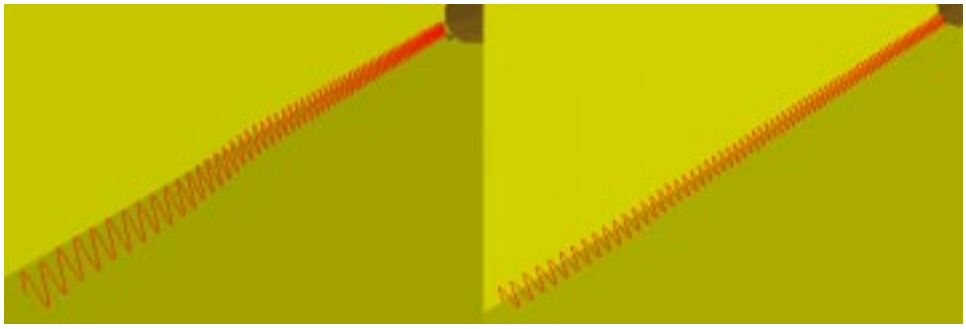

Figure 12: *Seam tracking with deviations of –20% (left) and –10% (right) in y and z directions, with K_a = 0.010, using the vector booster. The process is fully stable, and at –10% the convergence is good.*

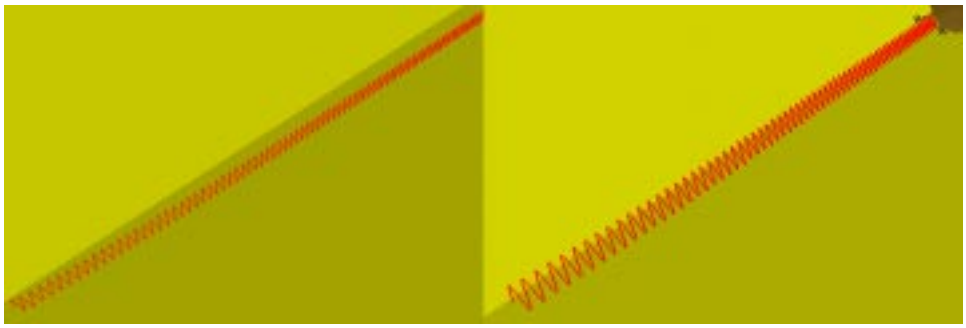

Figure 13: *The same as previous picture, but without the vector booster. As expected the convergence is even slower at –20% than before (left), but is still very good at –10% (right).*

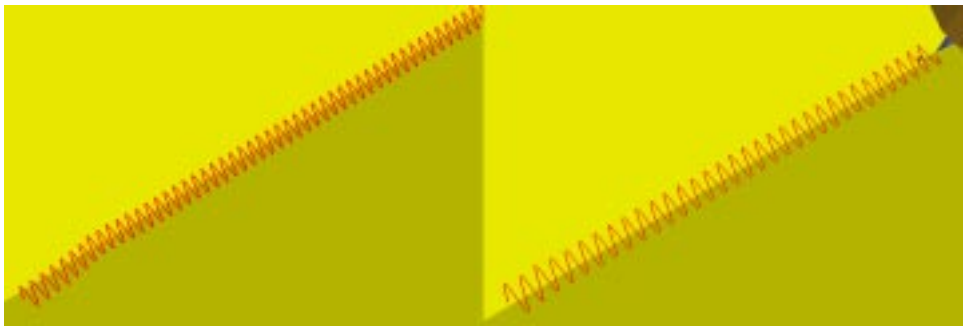

Figure 14: *Seam tracking with deviations of 30% (left) and 40% (right) in y and z directions with* K_a *= 0.010. There is no instability and the convergence is fine, but there is some clippings at 40%. The theoretical positive limit without using the vector booster is thus 30%.*

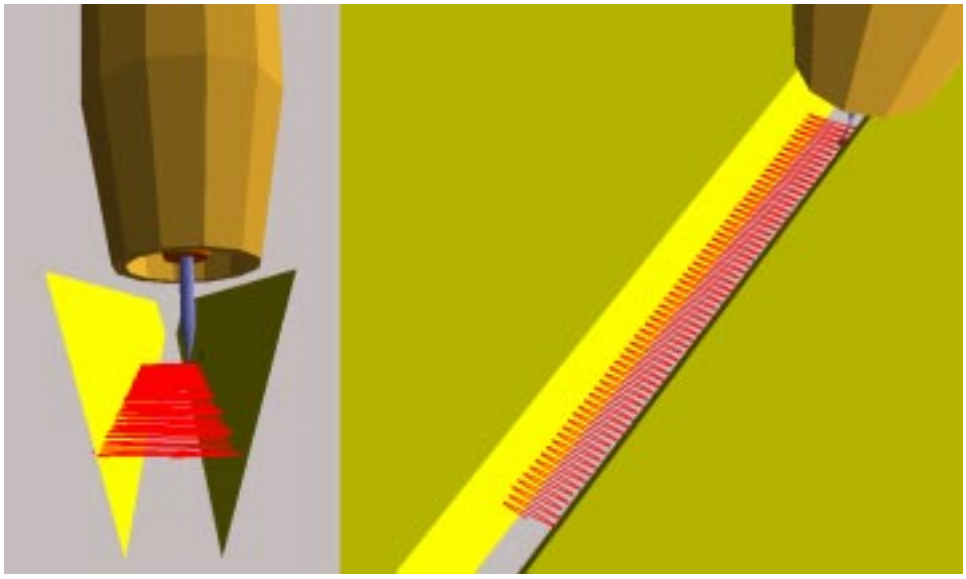

Figure 15: *Seam tracking with deviations of 20% in y and z directions, using the differential method with direct measurement in FUSE. K_a = 0.010. The process is stable and the convergence is fine.*

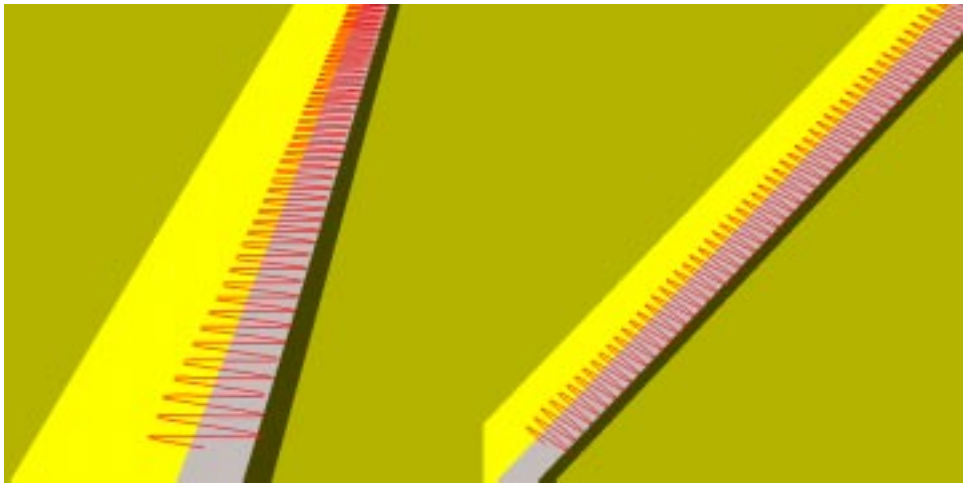

Figure 16: *Seam tracking with deviations of 20% in y and z directions, K_a = 0.010. The stability is high, but in the left picture the weaving is too near one of the walls. In the right picture convergence is fine, since the vector booster is used. In both experiments current calibration was used, which is default for the algorithm.*

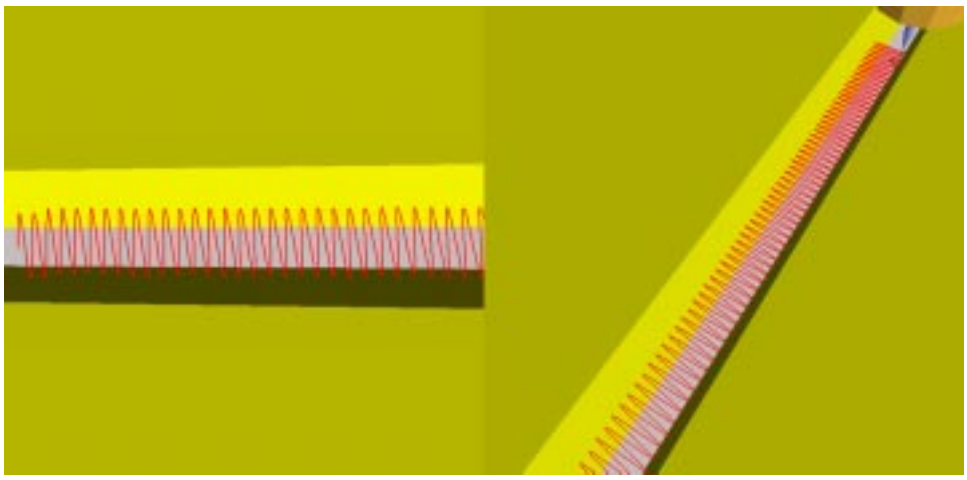

Figure 17: *Seam tracking with deviations of 10% (left) and –10% (right) in y and z directions. K_a = 0.010. Good results, but this are the limits in positive and negative directions.*

3.2 Validation by robot welding

3.2.1 Overview

Initial simulations showed that the algorithm used less than 1% of the computational power that it was assigned to, which equals 1/2000 of the total computational power of the real-time embedded system, so the efforts to produce efficient code was successful.

The simulation and validation loop described in Fig. 3 was repeated twice, and concluded with the evaluation simulations. The first physical experiments consisted of a number of fillet, V-groove and flat surface welds performed by the robot, with and without seam tracking. The primary task was to find the set of parameters for the power-source that resulted in good welding quality.

The second robot welding experiments performed on author request consisted of about 25 fillet and 25 V-groove joints. Also as a final evaluation of the implemented algorithm 10 fillet and 10 V-groove welds were carried out. In addition, an uncounted number of fillet and V-groove welds were performed to find good parameter settings for the power-source.

The overhead experiments showed to be many compared to the experiments specifically carried out by the directives of the author. About

Figure 18: *Example of fillet weld.*

Figure 19: *Example of V-groove weld. These workpieces are single sided and the seams have to be covered from the back by ceramic material to prevent welding flux from passing through the seams, and thereby cause low welding quality.*

120 fillet and 75 V-groove joint workpieces were estimated to have been used during the two experimental occasions. These overhead experiments showed to be very important for the development of the algorithm. Without precise parameter settings of the power-source, seam tracking would have worked, but without producing high-quality welds.

3.2.2 Anomalies caused by power-source

In theory, to be able to perform seam tracking at welding, the voltage and current of the power-source have to be expressed by some simple formula, such as Eq. 1. Usually the voltage is constant, while the current changes due to the distance between the wire and the workpiece.

In synergic welding however, both current and voltage are modified by the control system of the power-source, causing disruption in the control system of the algorithm. Early experiments with the Migatronic power-source using the pure synergic mode showed that the synergic mode disabled algorithm control in the negative approach direction of the TCP.

At the initial seam tracking experiments using the manual mode the current showed to constantly decrease throughout the weld, making compensation in the negative a-direction impossible. A thorough examination of the current sensor showed that the current measurements were both stable and sufficiently accurate for the application and that the decrease of current throughout the weld was not due to measurement errors. The conclusion was therefore that the Migatronic power-source controller was most likely controlling the current also at manual mode. The reason is assumed to be that modern power-sources also include some adaptive control in the manual mode to assist humans in performing high-quality welds. The compensation for the power-source control is henceforth called power-source compensation.

3.2.3 Compensation for power-source control

Addition of a constantly increasing offset to the nominal trajectory solved the problem caused by the adaptive behavior of the power-source. The solution had similarities with the vector booster method, but the modification of the trajectory increased constantly in negative direction of the approach axis.

To be able to handle negative deviations, K_a had to be doubled. The method was tested for fillet joints and showed to be a reliable and per-

manent solution to this problem. Since the same principal is valid for V-groove as fillet welds, no experimental series were considered necessary to prove the validity of the power-source compensation for V-groove welds. Thus the result of the experiments is that an algorithm that theoretically is able to produce an ideal quality weld, both for fillet and V-groove joints at seam tracking, has been developed and validated.

3.2.4 Power-source parameter settings

The following data was primarily acquired and logged during the second experimental series consisting of 80 fillet and V-groove experiments:

- objective,
- label,
- K_a, K_n,
- deviations in y and z directions,
- welding speed,
- weaving frequency and amplitude,
- weaving shape, see Fig. 20
- nominal voltage and current,
- wire speed,
- offset magnitude calculated by the vector booster, in x, y and z directions,
- a detailed description of the results.

The optimal parameters that were experimentally found giving high welding quality, are presented in Table 1.

3.2.5 Review of fillet welds

Example of typical fillet and V-groove samples are displayed in Figs. 18 and 19. Information from these initial experiments was used for the modification of the algorithm, followed by a new series of simulations. Some selected fillet and V-groove experiments are presented by photos

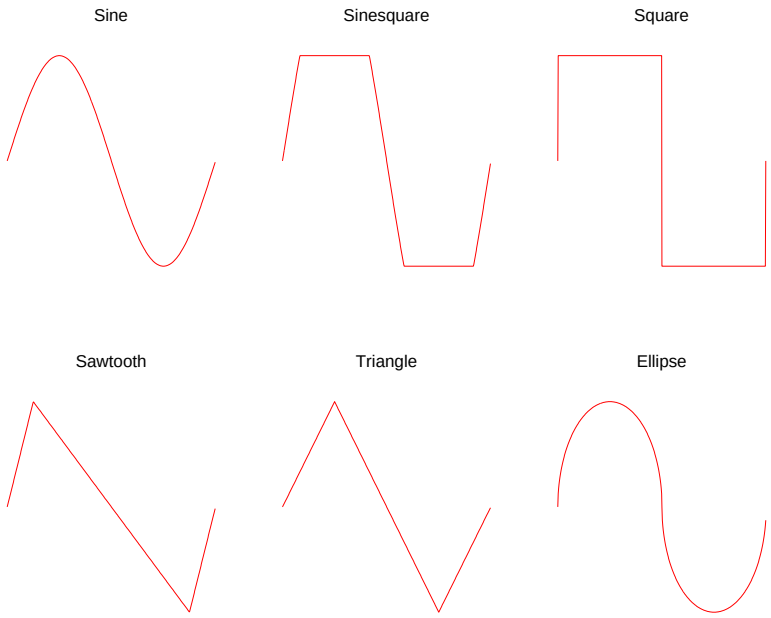

Figure 20: *The implemented weaving shapes in the algorithm. Sinesquare was chosen for fillet and sawtooth for V-groove welds for the achievement of maximum welding quality after a series of experiments and consultation with welding expertise. The sinesquare consists of a sine wave with an amplitude of 2 units, truncated at 1 unit.*

Parameter	Fillet weld	V-groove joint
Nominal voltage (V)	28	28.5
K_a	0.015	0.012
K_n	50% of K_a	50% of K_a
Weaving frequency (Hz)	3	2
Weaving shape	Sinesquare	Sawtooth
Welding speed (mm/s)	8	3.5
Wire speed (m/min)	9	7
Weaving amplitude (mm)	3	4

Table 1: *Recommended parameters using the Migatronic power-source, derived by experiments.*

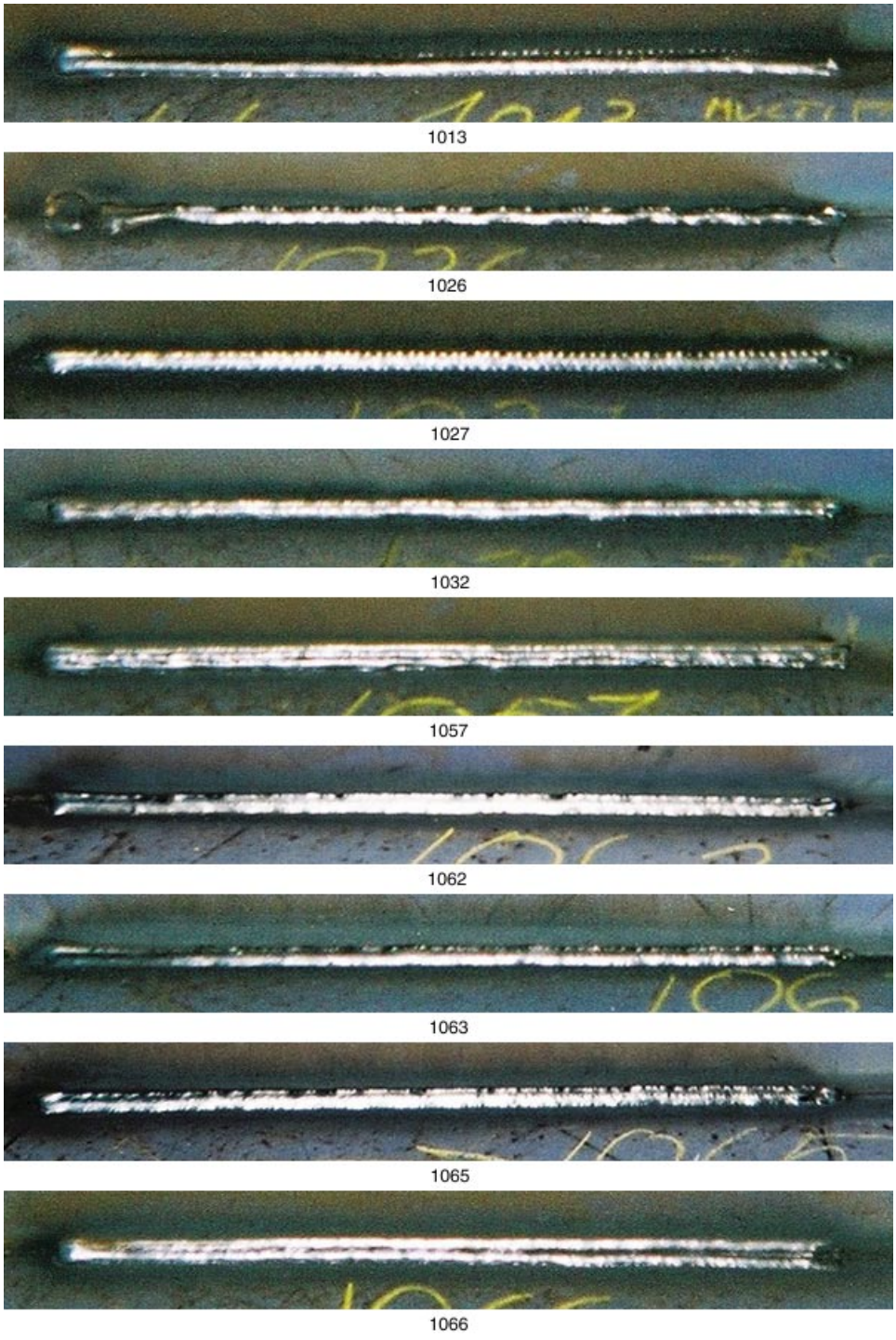

Figure 21: *Pictures of some selected fillet welds.*

in Figures 21 and 24. These experiments are further commented and reviewed below.

1013. Seam tracking and deviation in z direction by 8%, followed by multipass welding. Since the gains and the weaving frequency were too small, the seam tracking failed by a deviation of 2.3%. $K_a = 0.05$, $f = 1.5$ Hz.

1026. Seam tracking and deviation in y direction by 4%. K_n was too high and caused oscillations in the n direction, $K_a = 0.05$, $f = 3$ Hz.

1027. Reference welding without seamtracking, nearly optimal. $f = 3$ Hz, The distinct edges of the weaving indicate too high nominal voltage, cutting too deep into the workpiece.

1032. Seam tracking and deviation in both y and z directions by 8% each. High welding quality, but this is the limit for positive deviations. $K_a = 0.025$, $f = 3$ Hz.

1057. Seam tracking and a deviation of 2% in both y and z directions. High welding quality in both the root layer and multipass layers. $K_a = 0.0125$, $f = 3$ Hz.

1062. Final test. Seam tracking and a deviation of –2% in y direction, using power-source compensation. High welding quality. Remarks: the stick-out was 3 mm too large at the end of the seam and some instability occurred at the beginning of the seam. $K_a = 0.015$, $f = 3$ Hz.

1063. Final test. Seam tracking and a deviation of –2% in both y and z directions (specifications), using power-source compensation. High welding quality. Remarks: the stick-out was 3 mm too large throughout the seam. $K_a = 0.015$, $f = 3$ Hz.

1065. Final test. Seam tracking and a deviation of 2% in both y and z directions (specifications), using power-source compensation. High welding quality. Remarks: the stick-out was 3 mm too large in the end of the seam. $K_a = 0.015$, $f = 3$ Hz.

1066. Final test. Seam tracking and a deviation of 2% in both y and z directions (specifications), using power-source compensation, followed by multipass welding. High welding quality in the root layer. Remarks: the stick-out was 3 mm too large in the end of the seam, which had some effects for the multipass welding. Due to interference with the root layer, the last of the three layers deviated by 2 mm at the end of the seam from the root layer. $K_a = 0.015$, $f = 3$ Hz.

Additional information and summary of the selected fillet experiments in Fig. 21 follows below:

1. Higher weaving frequency gives in general faster control response

than lower. When the weaving frequency was increased from 1.5 Hz in 1013 to 3 Hz in 1032, the performance of the algorithm was more than doubled, where by performance is meant the maximum deviation error that the algorithm is able to compensate for, while maintaining high welding quality.

2. The experiments proved that K_n should be 50% or less than K_a, to avoid unstable control. This fact was previously discovered empirically at simulation.

3. In the presented fillet experiments, K_n was 50% of K_a in all cases except in 1013 where it was 75%. Due to problems in the newly developed robot system regarding the tuning of motor control, only a weaving frequency of 2-3 Hz could be used at most. At 3 Hz, the weaving amplitude was not able to exceed 3 mm despite the setting of 5 mm.

4. The fluctuation that occurred in the beginning of the seam in 1062, was due to the automatic calibration method that was applied. It was however found that the same main current value could be used as a reference point in the algorithm for all fillet welds. In future versions of the algorithm this feature will therefore not be used and the small fluctuation that sometimes occured in the beginning will be eliminated.

5. The wire stick-out was sometimes 3 mm larger than desired, according to the welding specialist. This does not effect the welding quality in the root layer, but may effect the multi-pass layers, since the subsequent layers interfere with the root layer. This interference is very small, only about 2 mm, but for high welding quality at multipass the algorithm should be fine-tuned to be able to reduce the stick-out some millimeters. One way to achieve this is to slightly increase the main current value. The power-source compensation factor should also be increased to avoid collision of the torch with the workpiece.

6. The most important experience from this experimental series was probably that the power-source compensation method showed to work properly.

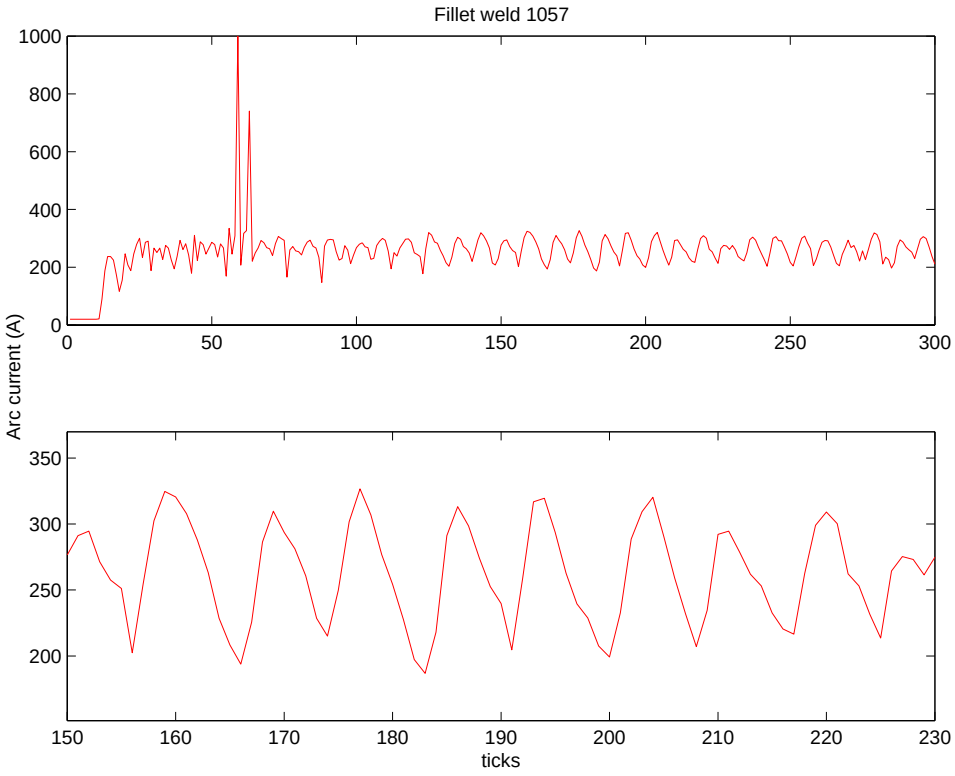

Figure 22: *Current samples from the first 6 seconds of a fillet weld experiment, using power-source compensation. The unit of the horizontal axis is ticks, which equals 1/50 seconds. The current values are filtered by an active 4:th order Bessel low-pass filter with f_0 = 10 Hz, added to the current sensor device, delivered from Migatronic. Though some transient spikes occurred in the initial part of the welding, the remaining data had relatively low level of noise. The lower figure is a magnification of a selected area of the upper.*

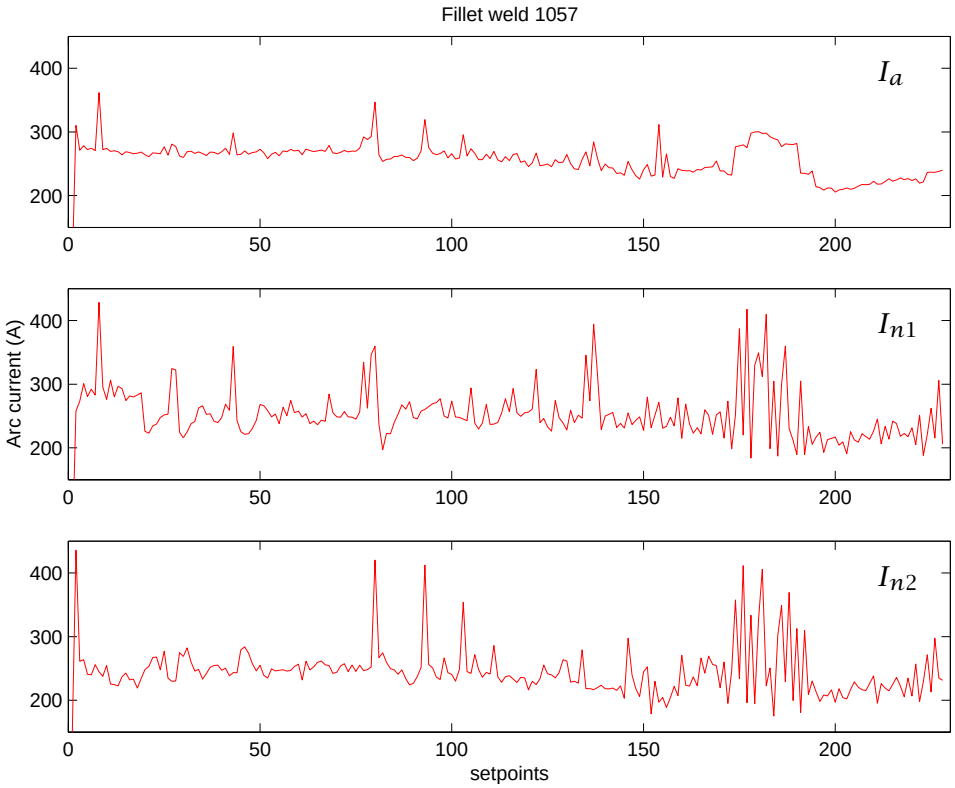

Figure 23: *Average current samples throughout the weld, using power-source compensation. The unit of the horizontal axis is setpoints, which in short welds is equal to one weaving cycle, but in longer is an integer multiple of weaving cycle. The upper figure displays I_a, which is the average current over each setpoint. The compensation in the TCP approach axis is made by multiplying this factor by the gain in a direction, K_a. In the middle and lower figures average currents I_{n1} and I_{n2} in the surroundings of the turning points of the weaving are displayed. The compensation in n direction is basically determined by K_n multiplied with the difference of I_{n1} and I_{n2}.*

3.2.6 Review of V-groove welds

Below follows comments and a review of the selected V-groove welding experiments presented in Fig. 24.

2031. Seam tracking and deviation in y direction by –2%. High welding quality. K_a = 0.015, f = 2 Hz.

2033. Seam tracking and deviation of 2% in y and z directions each. Seam tracking failed because of too small compensation, caused by the average current estimator. Observe that too long stickout, here about 10 mm too large, causes bubbles in the welds resulting in a low welding quality. K_a = 0.020, f = 2 Hz.

2041. Seam tracking and deviation of 2% in y and z directions each. High welding quality. A lower threshold value of 230 A has been added to the reference current estimator. Also anti-transient limiters have been added to the algorithm. K_a = 0.012, f = 2 Hz, U = 29 V.

2043. Final test. Seam tracking and deviation of 2% in y and z directions each. High welding quality. Basically the same experiment as above, except for U = 28.5 V, to enhance the welding quality. K_a = 0.012, f = 2 Hz.

2047. Final test. Seam tracking and deviation of 2% in y direction with two multipass layers on top of the root layer. High welding quality. K_a = 0.015, f = 2 Hz.

Since the power-source compensation showed to work according to the theory at fillet weld, the same was also assumed to be valid for V-groove welds, why due to prioritization of time in the ROWER-2 project, no additional experiments was considered as necessary.

4 Conclusions

The ROWER-2 specifications were fulfilled by the development and physical validation of a seam tracking algorithm distinguished by:

- Stable control in a and n-directions for fillet and V-groove joints (negative a-direction for V-grooves based on fillet weld experiments).
- Ability to perform multipass welding, both for fillet and V-groove joints, using interpolation.
- Maintaining high welding quality throughout the seam. This includes knowledge of the hoe to set the parameters of the power source.

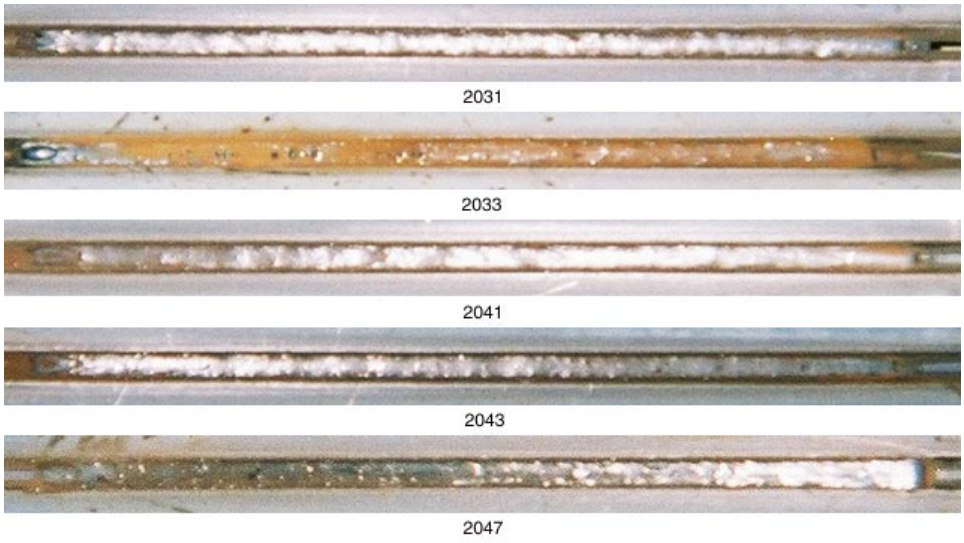

Figure 24: *Pictures of some selected V-groove welds.*

- Implementation of an auto-phase analyzer, calculating the total delay in the robot system, for optimal control. A new version of the FFT algorithm was designed and implemented in the auto-phase analyzer. This special version was faster and simpler to implement than an ordinary FFT for this specific task.
- Implementation of the vector booster method.
- Implementation of automatic current calibration at the start of the weld.

5 Acknowledgements

The ROWER-2 project is funded by European Commission under the BRITE/EURAM program.

References

[1] S. Adolfsson. *Simulation and execution of autonomous robot systems.* PhD thesis, Department of Production and Materials Engineering, Lund University, 1998.

[2] M. Arroyo Leon, A. Ruiz Castro, and R. Leal Ascencio. An artificial neural network on a field programmable gate array as a virtual sensor. In *Design of Mixed-Mode Integrated Circuits and Applications, 1999. Third International Workshop on*, pages 114–117, July 1999.

[3] P. Berbakov, D. MacLauchlan, and D. Stevens. Edge detection and seam tracking with emats. Patent No. US6155117, December 2000.

[4] G. Bolmsjö. Knowledge based systems in robotized arc welding. In *International Journal for the Joining of Materials*, volume 9 (4), pages 139–151, 1997.

[5] G. Bolmsjö. Sensor systems in arc welding. Technical report, Robotics Group, Department of Production and Materials Engineering, Lund University, Sweden, 1997.

[6] G. Bolmsjö. Programming robot welding systems using advanced simulation tools. In *Proceedings of the International Conference on the Joining of Materials*, pages 284–291, Helsingør, Denmark, May 16-19 1999.

[7] K. Brink, M. Olsson, and G. Bolmsjö. Increased autonomy in industrial robotic systems: A framework. In *Journal of Intelligent and Robotic Systems*, volume 19, pages 357–373, 1997.

[8] P. Cederberg, M. Olsson, and G. Bolmsjö. A generic sensor interface in robot simulation and control. In *Proceedings of Scandinavian Symposium on Robotics 99*, pages 221–230, Oulu, Finland, October 14-15 1999.

[9] G. E. Cook, K. Andersen, K. R. Fernandez, M. E. Shepard, and A. M. Wells. Electric arc sensing for robot positioning control. *Robot Welding*, pages 181–216. Editor: J. D. Lane. IFS Publications Ltd, UK, Springer-Verlag, 1987.

[10] W. Doggett and S. Vazquez. An architecture for real-time interpretation and visualization of structural sensor data in a laboratory environment. In *Digital Avionics Systems Conferences, 2000. Proceedings. DASC. The 19th*, volume 2, pages 6D2/1–6D2/8, Oct. 2000.

[11] M. Fridenfalk and G. Bolmsjö. The Unified Simulation Environment - Envision telerobotics and Matlab merged in one application. In *the Proceedings of the Nordic Matlab Conference*, pages 177–181, Oslo, Norway, October 2001.

[12] M. Fridenfalk, U. Lorentzon, and G. Bolmsjö. Virtual prototyping and experience of modular robotics design based on user involvement. In *the Proceedings of the 5th European Conference for the Advancement of Assistive Technology*, Düsseldorf, Germany, Nov. 1999.

[13] M. Fridenfalk, M. Olsson, and G. Bolmsjö. Simulation based design of a robotic welding system. In *Proceedings of the Scandinavian Symposium on Robotics 99*, pages 271–280, Oulu, Finland, October 14-15 1999.

[14] G. Ågren and P. Hedenborg. Integration of sensors for robot and welding power supply control. In *Proceedings of Fifth International Welding Computerization Conference*, pages 198–204, Golden, USA (AWS), August 1994.

[15] P. Hedenborg and G. Bolmsjö. Task control in robotics arc welding by use of sensors. In *Proceedings of the Tampere International Conference on Machine Automation - Mechatronics Spells Profitability, IFAC/IEEE*, pages 437–445, Tempre, Finland, February 15-18 1994.

[16] K. Hedengren and K. Haefner. Seam-tracking apparatus for a welding system employing an array of eddy current elements. Patent No. US5463201, October 1995.

[17] J. Huissoon and D. Strauss. System and method for tracking a feature on an object using a redundant axis. Patent No. US5465037, November 1995.

[18] L.-O. Larsson and G. Bolmsjö. A model of optical observable parameters to control robotic GMA welding in sheet steel. In *Proceedings of the Fifth International Conference on Computer Technology in Welding*, pages 2–10, paper 42, Paris, France, June 15-16 1994.

[19] M. Olsson. *Simulation and execution of autonomous robot systems*. PhD thesis, Division of Robotics, Department of Mechanical Engineering, Lund University, 2002.

[20] M. Oosterom and R. Babuska. Virtual sensor for fault detection and isolation in flight control systems - fuzzy modeling approach. In *Decision and Control, 2000. Proceedings of the 39th IEEE Conference on*, volume 3, pages 2645–2650, Dec. 2000.

[21] H. Pasika, S. Haykin, E. Clothiaux, and R. Stewart. Neural networks for sensor fusion in remote sensing. In *Neural Networks, 1999. IJCNN '99. International Joint Conference on*, volume 4, pages 2772–2776, July 1999.

[22] P. Ridao, J. Battle, J. Amat, and M. Carreras. A distributed environment for virtual and/or real experiments for underwater robots. In *Robotics and Automation, 2001. Proceedings 2001 ICRA. IEEE International Conference on*, volume 4, pages 3250–3255, May 2001.

[23] B. Rooks. Robot welding in shipbuilding. *The Industrial Robot*, 24(6):413–417, 1997.

[24] S. Sagatun and S. Hendseth. Efficient off-line programming of robot production systems. In *Proceedings of the 27th International Symposium on Industrial Robots. Robotics Towards 2000*, pages 787–792, CEU-Centro Esposizioni UCIMU, Cinisello Balsamo, Italy, 1996.

[25] P. Sorenti. Efficient robotic welding for shipyards—virtual reality simulation holds the key. *The Industrial Robot*, 24(4):278–281, 1997.

[26] Y. Suzuki. Method and apparatus for determining seam tracking control of arc welding. Patent No. EP1077101, February 2001.

[27] J. Villafuerte. Arc welding torch. Patent No. US6130407, October 2000.

[28] M. Xie and G. Bolmsjö. Using expert systems in arc monitoring and causal diagnosis in robotic arc welding. In *International Journal for the Joining of Materials*, volume 4 (4), 1992.

[29] M. Xie and G. Bolmsjö. Quality assurance and control for robotic GMA welding - part 1: QA model and welding procedure specification. In *Joining Sciences*, volume 1 (4), 1993.

[30] Yaskawa. *Arc Sensor COM-ARC III Instructions*.